

Experimental study on shear key restraint for earthquake

S.Fujimoto, H.Yoguchi & H.Hirayama

R & D Center, Toshiba Corporation, Kawasaki, Japan

A.Sakurai & Y.Masuko

Central Research Institute of Electric Power Industry, Abiko, Japan

1 Introduction

It is considered that a shear key restraint structure has potential of seismic suitability for a FBR. The shear key restraint structure is shown in Fig. 1. The shear key is put in a key way with a slight gap to allow thermal expansion discrepancy between a main vessel and a restraint structure. 24 shear key structures are arranged between the main vessel and the guard vessel. Then, stiffness for the main vessel increases, because the main vessel is connected with the guard vessel in a horizontal direction. As a result, the anti-earthquake performances of reactor components are improved by adopting this restraint structure.

Vibration characteristics as well as structural integrity of the shear key structures were investigated experimentally and analytically in this study, where the main vessel of pool-type LMFBR restrained by guard vessel using the shear key structures is selected as application example.

2 Vibration characteristics

2.1 Experimental Studies

2.1.1 Scale Model Structure A 1/10 scale model, in which the main vessel, the guard vessel and the shear key structures were simplified, was used (see Fig. 2) in order to investigate the effects of the shear key gap and the shear key stiffness on the load transfer characteristics of the shear keys and on the vibration characteristics of the main vessel. The similarity rule on dynamical properties between the scale model and the actual structures was applied. In the shear key model, two kinds of models, in which the shear key thickness differ, were considered to investigate the effects of the shear key stiffness. Rate of hard key stiffness (thickness 0.02 m) for soft key stiffness (0.014 m) is about 2.53. The masses of the main vessel model and the guard vessel model, containing the shear key structures, were 5.33×10^3 kg and 2.51×10^3 kg, respectively. The natural frequencies of the main vessel model and the guard vessel model were 9.15 Hz and 19.2 Hz, respectively.

2.1.2 Static Loading Test A hydraulic jack and a connection rod were used in order to investigate the effects of the shear key gap on

the load distributions acting on 22 shear keys, and the load-displacement relation of the main vessel model. Various key gaps, 0.0 , 1×10^{-4} , 2×10^{-4} and 3×10^{-4} m, were set up for the test. The load-displacement relation of the main vessel model for 0.02 m key thickness and 2×10^{-4} m key gap case is shown in Fig. 3. The load distributions (shear force) in the shear keys for a 6.86×10^4 N load are shown in Fig. 4.

2.1.3 Vibration Test In this test, sinusoidal wave vibration tests and random wave vibration tests were performed by using a large earthquake simulator. In the scale model, the connection rod were detached. The time histories of the sinusoidal wave input, the response acceleration of the main vessel model and the guard vessel model, and the 90° shear key force for the 2×10^{-4} m shear key gap case are shown in Fig. 5. The resonant frequencies of the main vessel model for the acceleration amplitude of the sinusoidal sweep input are shown in Fig. 6. The relations between the maximum response acceleration of the main vessel model and the maximum random wave input acceleration are shown in Fig. 7. Furthermore, the maximum load distributions of the shear keys (0.02 m key thickness) for the random vibration wave input are shown in Fig. 8. The broken line shows the load distribution of the shear key in the static loading test.

2.2 Analytical Studies

Dynamical response analyses for the scale model tests were performed by using a analytical model in which the FBR structure with shear key structures were simplified. The analytical model (see Fig. 9) is assumed as follows.

- (1) The shear key structures are expressed by linear springs and dampers with gaps.
- (2) The overall shell deformation of the main vessel and the guard vessel are neglected. Then, the main vessel and the guard vessel are expressed by a single-degree-of-freedom system with an equivalent linear spring and mass.
- (3) The shear key gap in the vibration direction is given as an equivalent gap depending on the arrangement angle.

Numerical simulation results are shown as follows. The time history of the responses of the main vessel model and the guard vessel model, and the shear key force of the 90° shear key for the sinusoidal wave input in Fig. 5 are shown in Fig. 10. The experimental and analytical load distributions of the shear keys for the same sinusoidal wave input are shown in Fig. 11. The analytical results and the experimental results agree well.

2.3 Results

From the experimental and analytical studies, the following has been made clear:

- (1) As the shear key gap becomes large, the shear key loads in the neighborhood of 90° and 270° increase for the same jack load. The increase rate of the 90° and 270° shear key load in the case of a 3×10^{-4} m key gap is about 30 % for key gap 0.0 m case.
- (2) Dynamic load distributions and static load distributions of the shear keys agree well.
- (3) No complicated phenomenon caused by a dynamic input (ex. impact responses) could be found out. That is, a local collision phenomenon in the shear key can be neglected and the shear key is consid-

ered approximately to be a static spring.

- (4) The analytical method can be sufficiently valuable for the seismic response prediction of the main vessel and the shear key loads.

3 Structural Integrity

Static tests were conducted to investigate the structural integrity of this type of shear key restraint using 1/3-scale models. The purpose of these tests were to evaluate the maximum load, fracture mode and safety margin of the design condition.

3.1 Test Models and Loading Conditions

In the seismic analysis of pool-type LMFBR with a shear key restraint, it was observed that circumferential moment resultants and radial displacement caused by the reaction forces of shear key were asymmetric with respect to the shear key center and nearly equal to zero at the key center of two adjacent keys. Therefore test model covered one pitch of actual structure (15° sector) having a key and key way at the center of it. To balance the test load, two pairs of main vessel and guard vessel made of 304 stainless steel were located symmetrically as shown in Fig. 12. The bottom ends of guard vessels were fixed on the base and top faces of main vessels were loaded downward. Displacement and strain distributions were measured at over 280 points.

3.2 Test Results

Figure 13 shows the load-displacement curve of main vessel measured at the bottom face. As load increased, key and key way exhibited a remarkable plastic deformation, and after a load attained the maximum value, two keys slid down on the key way surfaces. The maximum loads for two models were $245 \times 10^4 \text{N}$ and $248 \times 10^4 \text{N}$ (about $123 \times 10^4 \text{N}$ for each pair of key and key way). The design load for actual size of each key and key way was $218 \times 10^4 \text{N}$ ($24 \times 10^4 \text{N}$ for 1/3-scale model estimated by the similarity rule), and so, the safety margin of 5.1 was obtained by these tests. The residual deformations of these models are shown in Fig. 14. The bending angles were about $104 - 112^\circ$ and no part of these model was damaged except for the above mentioned deformation. The failure mode of this shear key restraint was considered to be a kind of typical plastic collapse. Load-strain curves at the root of the shear key and longitudinal stress distributions of main vessel are shown in Figs. 15 and 16. From the measured strain distributions in Fig. 15, it was clarified that the strain was concentrated at the root of the key and also key way and the above stated plastic deformation occurred mainly at these portions. As shown in Fig. 16, the stress distributions for each load step were also asymmetric with respect to the key center, and so, the results using these models gave us the correct deformation characteristics.

4 Conclusion

From the analytical and experimental studies, the vibration characteristics and the structural integrity of the shear key structures were made clear. Further, valuable data for the design of the shear key structures were obtained.

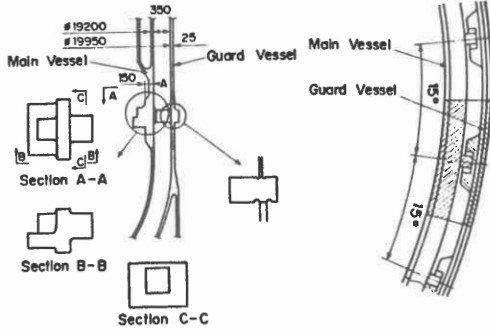


Fig.1 Shear key structure for pool type LMFBFR

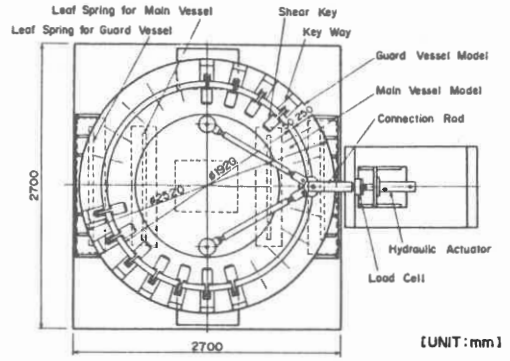


Fig.2 Scale model of FBR structure with shear keys

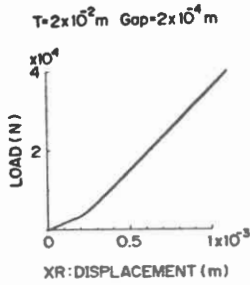


Fig.3 Load-displacement relation of main vessel model

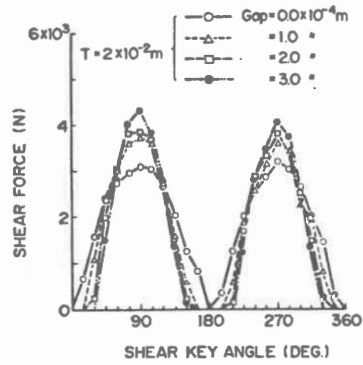


Fig.4 Load distributions of shear keys (statical loading test)

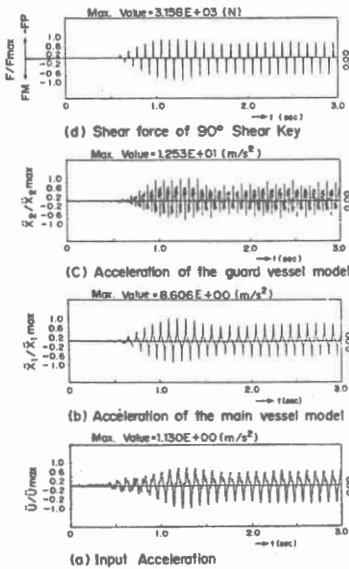


Fig.5 Time history of input and scale model responses ($T=2 \times 10^{-2} \text{ m}$, $\text{Gap}=2 \times 10^{-4} \text{ m}$)

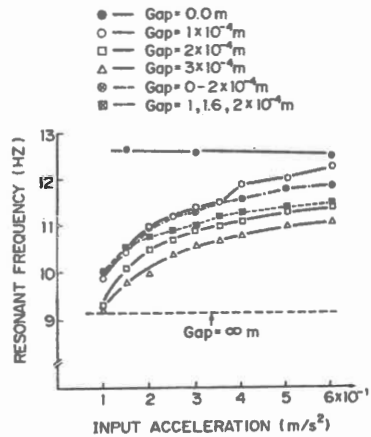


Fig.6 Resonant frequency of main vessel model for input level

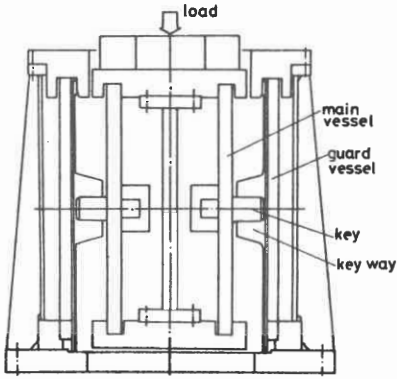


Fig.12 Assembly of structural integrity test model for shear key restraint

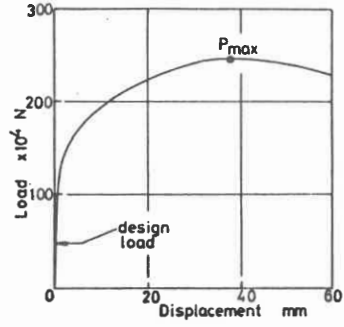


Fig.13 Load-displacement curve of main vessel

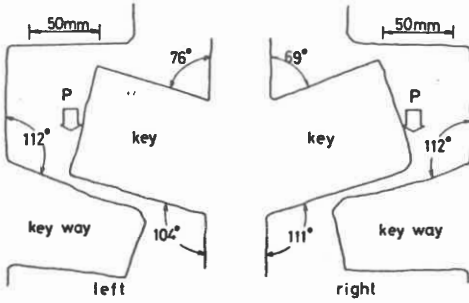


Fig.14 Residual deformation of keys and key ways

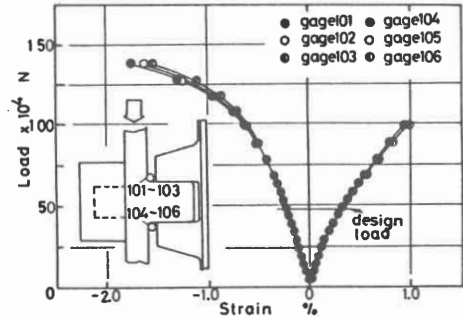


Fig.15 Strain distributions at the root of key

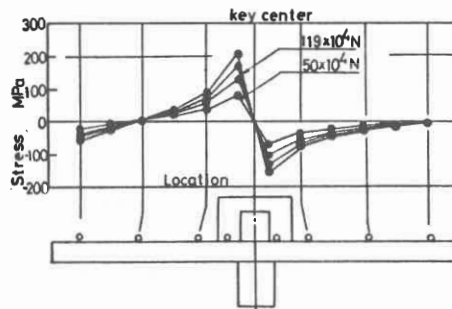


Fig.16 Longitudinal stress distributions of main vessel